Structural Changes in Tritium-Substituted Polymeric Materials by Beta Decays: A Molecular Dynamics Study*)

Haolun LI, Susumu FUJIWARA, Hiroaki NAKAMURA[1,2)], Tomoko MIZUGUCHI, Takuo YASUNAGA[3)], Takao OTSUKA[4)], Takahiro KENMOTSU[5)], Yuji HATANO[6)] and Shinji SAITO[7)]

Graduate School of Science and Technology, Kyoto Institute of Technology, Kyoto 606-8585, Japan
[1)]*Graduate School of Engineering, Nagoya University, Nagoya 464-8601, Japan*
[2)]*National Institute for Fusion Science, National Institutes of Natural Sciences, Toki 509-5292, Japan*
[3)]*Kyushu Institute of Technology, Iizuka 820-8502, Japan*
[4)]*RIKEN, Wako 351-0198, Japan*
[5)]*Doshisha University, Kyotanabe 610-0394, Japan*
[6)]*University of Toyama, Toyama 930-8555, Japan*
[7)]*Institute for Molecular Science, National Institutes of Natural Sciences, Okazaki 444-8585, Japan*

(Received 10 January 2019 / Accepted 10 April 2019)

The molecular mechanism through which how beta decays in tritium-substituted species damage DNA and polymeric materials is still unknown. Molecular dynamics simulations of hydrogen-removed polyethylene were performed to predict the structural change of the polyethylene chain after the substituted tritium decays. We calculated the potential energy, the global orientational order parameter, and the average number of consecutive *trans* bonds. The results are that, the greater the number of removed hydrogen atoms, the higher the potential energy and the lower the value of the global orientational order parameter and the average number of consecutive *trans* bonds. Thus, after losing hydrogen, polyethylene becomes poorer in terms of both thermal and structural stabilities.

Keywords: polyethylene, molecular dynamics simulation, beta decay, structural change, tritium

DOI: 10.1585/pfr.14.3401106

1. Introduction

Following the Fukushima nuclear accident in 2011, a large amount of tritiated water was discharged, which caused high levels of pollution to the surrounding land and the sea. Tritiated water is a type of water which contains tritium (T or ^{3}H), a radioactive isotope of hydrogen. With a half-life of 12.323 years, tritium decays to helium-3 (^{3}He) by beta decay with emissions of a beta-electron (beta-ray) and an antineutrino [1]. In particular, on macromolecules, such as DNA and polymeric materials, beta-rays may cause damage, and if substituted tritium decays to helium-3, chemical bonds break, destabilizing the structure. However, the molecular mechanism of this damage caused by tritium is still an unsolved problem. Therefore, our aim is to predict the structural change of tritium-substituted macromolecules, such as DNA and polymeric materials, by beta decays of tritium to helium-3 using molecular dynamics (MD) simulations.

In this paper, MD simulations of polyethylene were performed to study the structural change of polyethylene by beta decays of substituted tritium.

2. Model and Simulation

The polyethylene model is made up of a linear chain of 2998 CH_2 groups with two terminal CH_3 groups all treated as united atoms, with masses of 14 and 15 g/mol, respectively. After decay of substituted tritium to helium-3, the C–T bonds break, as the inert helium-3 is freed. To imitate the decay effect on the polymer chain, hydrogen atoms are removed randomly from the polyethylene. The remaining -CH- united atoms, with a mass of 13 g/mol, are considered overlapping sp^2 hybrid orbitals [2]. The ratio of the number of removed hydrogen atoms to the number of carbon atoms, f_H, is set at f_H = 0, 0.001, 0.01 and 0.1.

The DREIDING potential [3] is the generic force field used in this research, which is useful for predicting structures and dynamics of polymers. As atom types of the DREIDING force field, a label such as "C_32" is used to stand for each type of united atom. The first two characters correspond to the chemical elements (e.g., "He" for helium), where an underscore is added for elements with only one letter (e.g., "C_" for carbon). The third character suggests the hybridization: 1 for linear (sp^1), 2 for trigonal

author's e-mail: m8672034@edu.kit.ac.jp
*) This article is based on the presentation at the 27th International Toki Conference (ITC27) & the 13th Asia Pacific Plasma Theory Conference (APPTC2018).

Table 1 Equilibrium bond distance R^0_{IJ}, where "C_3" includes both "C_33" and "C_32", and "C_2" represents "C_21".

I	J	R^0_{IJ} (Å)
C_3	C_3	1.53
C_3	C_2	1.43
C_2	C_2	1.33

Table 2 Equilibrium angle θ^0_J, where "C_3" includes both "C_33" and "C_32", and "C_2" represents "C_21".

J	θ^0_J (deg)
C_3	109.471
C_2	120.000

(sp^2), and 3 for tetrahedral (sp^3). The fourth character indicates the number of implicit hydrogen atoms. As part of a united atom, hydrogen atoms are not to be calculated independently. Therefore, there are three atom types used in this paper: "C_33" for the CH_3 group, "C_32" for the CH_2 group, and "C_21" for the -CH- group, which is generated by removing a hydrogen atom from the CH_2 group.

The potential energy (1) includes bonded interactions ($E_{\rm val}$) and nonbonded interactions ($E_{\rm nb}$):

$$E_{\rm pot} = E_{\rm val} + E_{\rm nb}. \tag{1}$$

In this paper, $E_{\rm val}$ (2) consists of the sum of bond stretch ($E_{\rm B}$), bond-angle bend ($E_{\rm A}$), and dihedral angle torsion ($E_{\rm T}$),

$$E_{\rm val} = E_{\rm B} + E_{\rm A} + E_{\rm T}, \tag{2}$$

whereas $E_{\rm nb}$ is the Lennard–Jones potential:

$$E_{\rm nb} = E_{\rm LJ}. \tag{3}$$

The bond stretch interaction ($E_{\rm B}$) is given by the expression (4)

$$E_{\rm B} = \frac{1}{2}K_{IJ}(R_{IJ} - R^0_{IJ})^2, \tag{4}$$

where R_{IJ} is the bond distance between atom I and atom J. The force constant is K_{IJ} = 700 (kcal/mol)/Å^2. R^0_{IJ} is the equilibrium bond distance, and Table 1 shows the values of R^0_{IJ}.

The angle bend interaction is calculated using Eq. (5):

$$E_{\rm A} = \frac{1}{2}K_{IJK}(\theta_{IJK} - \theta^0_J)^2, \tag{5}$$

where θ_{IJK} is the angle between bonds IJ and JK, and the force constant is K_{IJK} = 100 (kcal/mol)/rad^2 for the angle bend. θ^0_J represents the equilibrium angle. The values of θ^0_J are given in Table 2.

The torsion interaction (6) takes the form

Table 3 Parameters used for the torsion interaction.

J	K	V_{JK} (kcal/mol)	n_{JK}	φ^0_{JK} (deg)
C_32	C_32	2.0	3	180
C_32	C_21	1.0	6	0
C_21	C_21	45	2	180

Table 4 Parameters used for the Lennard–Jones potential.

I	J	ε (kcal/mol)	σ (Å)
C_32	C_32	0.1984	3.6239
C_33	C_33	0.2500	3.6994
C_32	C_33	0.2227	3.6616
C_21	C_21	0.1450	3.5458
C_21	C_32	0.1696	4.0677
C_21	C_33	0.1904	4.1524

$$E_{\rm T} = \frac{1}{2}V_{JK}\{1 - \cos[n_{JK}(\varphi - \varphi^0_{JK})]\}, \tag{6}$$

where φ is the dihedral angle between the planes IJK and JKL, V_{JK} is taken as the energy barrier to rotation, n_{JK} is the periodicity, and φ^0_{JK} is the equilibrium angle. As V_{JK}, n_{JK}, and φ^0_{JK} are independent of atom I and atom L, the values are as shown in Table 3.

For the Lennard–Jones potential as a nonbonded interaction, the common Eq. (7) is used:

$$E_{\rm LJ}(r) = 4\varepsilon\left[\left(\frac{\sigma}{r}\right)^{12} - \left(\frac{\sigma}{r}\right)^{6}\right], \tag{7}$$

with a cutoff of 10.5 Å, where r is the distance between two united atoms, ε is the depth of the potential well and σ is the finite distance at which the interparticle potential is zero. Table 4 shows the values of ε and σ.

By using the velocity version of the Verlet algorithm [4], the equations of motion for all united atoms are solved numerically. To keep the temperature of the system constant, the Nosé–Hoover method is applied [5–7]. The integration time step is 1 fs.

Three different simulation runs are performed for each $f_{\rm H}$ as follows. First, for preparation, the isolated polyethylene is cooled from 800 to 300 K, at a rate of 50 K/ns (10,000,000 time steps or 10 ns in total) in a vacuum simulation box, forming a folded, orientationally ordered structure, in agreement with S. Fujiwara and T. Sato [8]. Secondly, hydrogen atoms are randomly removed from the polyethylene model for three simulation runs. For $f_{\rm H}$ = 0, the simulations are run for an extra 1,000,000 and 2,000,000 time steps (1 ns and 2 ns, respectively) at 300 K as a preparation for the second and third simulation runs, respectively. After that, the model is heated stepwise to 550 K, at a rate of 10 K/ns (1,000,000 time steps at each

temperature, 25,000,000 time steps or 25 ns in total), and the model still maintains a folded, orientationally ordered structure at 550 K. Then, the temperature of the simulation box undergoes a second stepwise increase, to 800 K, at the low rate of 2 K/ns (1,000,000 time steps at each temperature, 125,000,000 time steps or 125 ns in total). All the simulations were run using LAMMPS [9, 10].

3. Results and Discussion

3.1 Structural changes

Structures were visualized using the VMD software [11, 12]. Structural changes in all models are observed, from an orientationally ordered structure to a disordered one. Figures 1 and 2 show the structure of the models for one of the simulation runs before and after the structural change at a certain temperature of 650 and 700 K, respectively. In the latter, the main chains are shown in blue lines, whereas -CH- groups are shown in red balls.

3.2 Potential energy

As mentioned in Section 2, the potential energy is calculated using Eqs. (1) - (7), and Fig. 3 shows the average curves obtained for three different simulation runs.

It can be seen from Fig. 3 that curves for $f_H = 0$, $f_H = 0.001$ and $f_H = 0.01$ are similar, although E_{pot} at $f_H = 0.1$ is the largest among the range of f_H tested. E_{pot} for $f_H = 0.1$ increases sharply from about 650 to 690 K, whereas the sharp increase of E_{pot} for other f_H's starts at about 650 K and remains up to about 720 K. Above 720 K, all E_{pot} curves converge to a linearity, in a similar fashion. This observation can be interpreted as follows. We find that during heating, the values of E_B for different values of f_H are almost the same, as well as the values of E_A and E_T. However, the values of E_{LJ} for different values of f_H are different. In the temperature range where the structure changes, the difference of E_{LJ} becomes maximum, whereas over 720 K, E_{LJ} becomes almost the same, once the obtained structure is disordered. As a result, the E_{pot} ($= E_B + E_A + E_T + E_{LJ}$) over 720 K becomes identical.

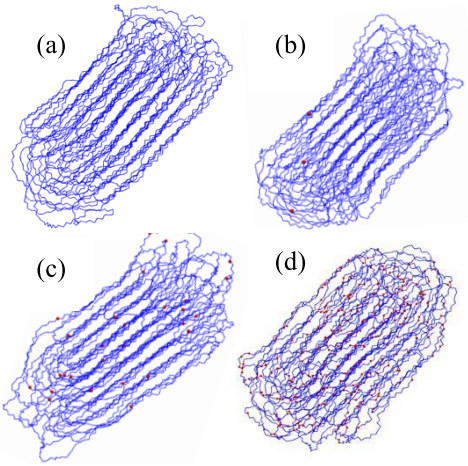

Fig. 1 Side views of polyethylene at 650 K for (a) $f_H = 0$, (b) $f_H = 0.001$, (c) $f_H = 0.01$, (d) $f_H = 0.1$.

3.3 Global orientational order parameter

The global orientational order parameter (P_2) is calculated using expression (8) to analyze the degree of orientational order in the polyethylene chain as

$$P_2 = \left\langle \frac{3\cos^2\Psi - 1}{2} \right\rangle_{\text{bond}}, \tag{8}$$

where Ψ is the angle between two chord vectors and $\langle \cdots \rangle_{\text{bond}}$ denotes the average among all pairs of chord vectors. Here the chord vector is defined as the vector from the center of one bond to the center of another adjacent bond along the polymer chain. When all chord vectors are parallel, $P_2 = 1$, and when all chord vectors are randomly oriented, $P_2 = 0$. Figure 4 shows the dependence of P_2 on temperature T for all f_H's.

For $f_H = 0$, P_2 decreases most quickly at the increasing temperatures from about 665 to 695 K, whereas for $f_H \neq 0$, P_2 drops from 665, 660, 640 K to about 690, 690, 670 K for $f_H = 0.001$, $f_H = 0.01$, and $f_H = 0.1$, re-

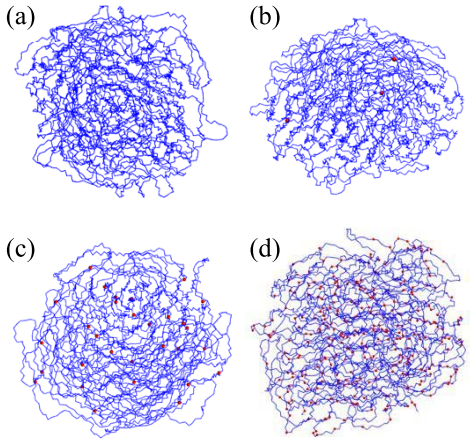

Fig. 2 Side views of polyethylene at 700 K for (a) $f_H = 0$, (b) $f_H = 0.001$, (c) $f_H = 0.01$, (d) $f_H = 0.1$.

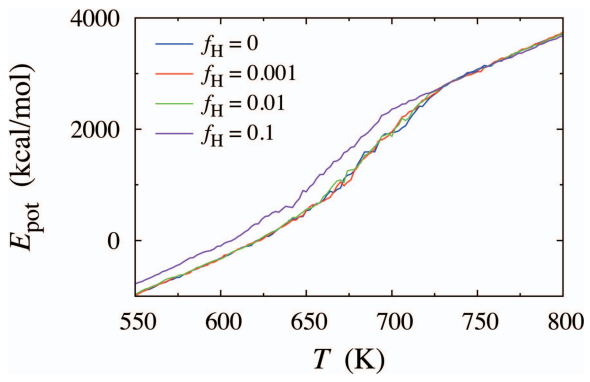

Fig. 3 Temperature dependence of the potential energy E_{pot} for (a) $f_H = 0$, (b) $f_H = 0.001$, (c) $f_H = 0.01$, (d) $f_H = 0.1$.

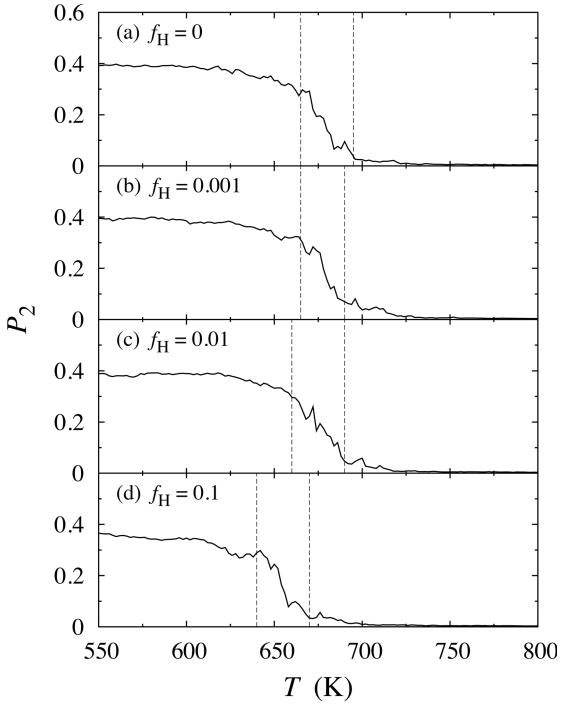

Fig. 4 Temperature dependence of P_2 for (a) $f_H = 0$, (b) $f_H = 0.001$, (c) $f_H = 0.01$, (d) $f_H = 0.1$.

spectively. It can be found from the temperature range in which such curves drop that the greater the value of f_H is, the ordered structure breaks down at lower temperatures. For all values of f_H, there is a clear P_2 residual after the main drop, which does not hold for long, disappearing at about 720 K.

3.4 Conformational change

Moreover, all local structures, consisting of several united atoms, were checked to investigate conformational changes. As the values of the dihedral angle φ were examined, the *trans* state and the *gauche* state were defined by $|\varphi| \leq \pi/3$ and $|\varphi| > \pi/3$, respectively [8].

The average size of *trans* segments, i.e., the average number of consecutive *trans* bonds $\overline{n_{tr}}$, was calculated and are shown in Fig. 5. The curves of $\overline{n_{tr}}$ are the average of three simulation runs. $\overline{n_{tr}}$ corresponds to the persistence length, which fits to the following relation (9) at high temperatures:

$$\overline{n_{tr}} \propto \exp\left(\frac{\Delta\varepsilon}{k_B T}\right), \tag{9}$$

where $\Delta\varepsilon$ is the torsional energy barrier between the *trans* and the *gauche* conformations and k_B is the Boltzmann constant.

As Fig. 5 shows, the values of $\overline{n_{tr}}$ for $f_H = 0$, $f_H = 0.001$, and $f_H = 0.01$ are at the same level, whereas the values of $\overline{n_{tr}}$ for $f_H = 0.1$ are smaller. The curves increase sharply with decreasing temperature at about 720 K for $f_H = 0$, $f_H = 0.001$, and $f_H = 0.01$ and at about 690 K for

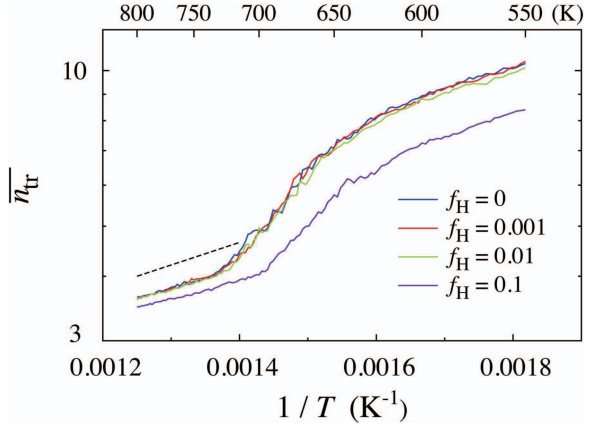

Fig. 5 The average size of the *trans* segments $\overline{n_{tr}}$ vs inverse temperature $1/T$ for (a) $f_H = 0$, (b) $f_H = 0.001$, (c) $f_H = 0.01$, (d) $f_H = 0.1$. The dashed line is the line fitted for high temperature region by Eq. (9) with $\Delta\varepsilon = 2.0$ kcal/mol.

$f_H = 0.1$. The curves are well fitted by Eq. (9) at the high temperature range over 700 K, with $\Delta\varepsilon = 2.0$ kcal/mol, which is the value of V_{JK} for torsion interaction between C_32 and C_32 in Eq. (6).

4. Conclusions

In this research, the structural changes of tritium-substituted polyethylene with three types of united atoms by beta decays of tritium to helium-3 have been studied during the gradual stepwise heating by MD simulations.

All models kept a folded, orientationally ordered structure at first, which became gradually disordered upon heating. As f_H becomes larger, it is found that:

(i) The visualized structure is more disordered at the same temperature what is also reflected in the lesser value of P_2 for a greater f_H.
(ii) The change of ordered structure starts and ends at a lower temperature for a greater value of f_H.
(iii) In Figs. 3 - 5, the curves change at the same temperature range for each f_H, respectively. Such range can be regarded as the range where the structural changes are occurring for each f_H.

The results suggest that both the thermal and structural stabilities of polyethylene can be decreased by removing hydrogen atoms from the chain. The greater the number of removed hydrogen atoms, the clearer the effect. We also find that the curves of physical quantities (E_{pot}, P_2, and $\overline{n_{tr}}$) of each simulation run are slightly different in shape from other simulation runs, suggesting that the positions of the removed hydrogen atoms have an effect on the structure.

In a future work, ReaxFF (Reactive Force Field) MD simulation studies will be performed to treat all hydrogen atoms and residual electrons properly.

Acknowledgments

This study was partially supported by the Joint Studies Program (2017 - 2019) of the Institute for Molecular Science, the Joint Research by the National Institutes of Natural Sciences (NINS), JSPS KAKENHI Grant Number JP15K05244, and the NIFS Collaborative Research Program (NIFS17KNTS050).

[1] T. Tanabe (ed.), *Tritium: Fuel of Fusion Reactors* (Springer Japan, Japan, 2017).
[2] S. Fujiwara, H. Nakamura, H. Li, H. Miyanishi, T. Mizuguchi, T. Yasunaga, T. Otsuka, Y. Hatano and S. Saito, Adv. Simulat. Sci. Eng. **6**, 94 (2019).
[3] S.L. Mayo, B.D. Olafson and W.A. Goddard III, J. Phys. Chem. **94**, 8897 (1990).
[4] W.C. Swope, H.C. Andersen, P.H. Berens and K.R. Wilson, J. Chem. Phys. **76**, 637 (1982).
[5] S. Nosé, Mol. Phys. **52**, 255 (1984).
[6] S. Nosé, J. Chem. Phys. **81**, 511 (1984).
[7] W.G. Hoover, Phys. Rev. A **31**, 1695 (1985).
[8] S. Fujiwara and T. Sato, J. Chem. Phys. **114**, 6455 (2001).
[9] https://lammps.sandia.gov/
[10] S. Plimpton, J. Comp. Phys. **117**, 1 (1995).
[11] https://www.ks.uiuc.edu/Research/vmd/
[12] W. Humphrey, A. Dalke and K. Schulten, J. Molec. Graphics **14**, 33 (1996).